Smart Vaults: Thermally-Responsive Protein Nanocapsules

Nicholas M. Matsumoto,[†] Panchami Prabhakaran,[†] Leonard H. Rome,[‡] and Heather D. Maynard[†,*]

[†]Department of Chemistry and Biochemistry and California Nanosystems Institute, 607 Charles E. Young Drive East, University of California, Los Angeles, California 90095-1569, United States and [‡]Department of Biological Chemistry, David Geffen School of Medicine and California Nanosystems Institute, University of California, Los Angeles, California 90095, United States

ABSTRACT Synthetic modification of a recombinant protein cage called a vault with stimuli-responsive smart polymers provides access to a new class of biohybrid materials; the polymer nanocapsules retain the structure of the protein cage and exhibit the responsive nature of the polymer. Vaults are naturally occurring ubiquitous ribonucleoprotein particles $41 \times 41 \times 72.5$ nm composed of a protein shell enclosing multiple copies of two proteins and multiple copies of one or more small untranslated RNAs. Recombinant vaults are structurally identical but lack the vault content.

Poly(N-isopropylacrylamide) (pNIPAAm), a polymer responsive to heat, was conjugated to recombinant vaults that were composed of ~78 copies of the major vault protein (MVP) modified to contain a cysteine rich region at the N-terminus (CP-MVP). The polymer was synthesized using reversible addition—fragmentation chain transfer (RAFT) polymerization to have a dansyl group at the alpha end and modified to have a thiol-reactive pyridyl disulfide at the omega end, which readily coupled to CP-MVP vaults. The resulting vault nanocapsules underwent reversible aggregation upon heating above the lower critical solution temperature (LCST) of the polymer as determined by electron microscopy (EM), dynamic light scattering experiments, and UV—vis turbidity analysis. The vault structure remained entirely intact throughout the phase transition; suggesting its use in a myriad of biomedical and biotechnology applications.
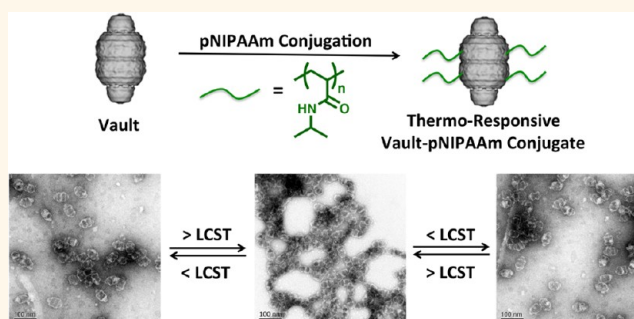
KEYWORDS: vault · protein cage · thermo-responsive · protein—polymer conjugate · poly(N-isopropylacrylamide)

Naturally derived protein cages, such as virus capsids and ferritin, serve as excellent templates for functional biohybrid materials with precise architectures, unattainable by purely synthetic processes.[1−5] Such materials have been developed for applications in the fields of nanotechnology,[4,6] biotechnology,[5,7] electronic materials,[8,9] catalysis,[10−12] and drug delivery.[13−16] The regular arrangement of protein subunits within protein cage structures allows for synthetic modification of specific regions and surfaces of the protein cage, such as the exterior shell or interior cavity. The conjugation of synthetic polymers to viruses, such as adenovirus, cowpea mosaic virus, tobacco mosaic virus, and others has been investigated.[17−20] For example, poly(ethylene glycol) has been attached to adenovirus and cowpea mosaic virus and has been shown to decrease immunogenicity of the particles.[17,19] Recently, Douglas and co-workers have polymerized

2-aminoethyl methacrylate from the interior of P22 capsids creating a particle capable of encapsulating magnetic resonance imaging (MRI) contrast agents.[21] Although there are several examples of polymer conjugation to protein cages, to our knowledge there are no examples of stimuli-responsive smart polymers conjugated to protein cages. Yet such materials can reversibly alter the physical characteristics of the nanobiomaterial by an externally controlled trigger.
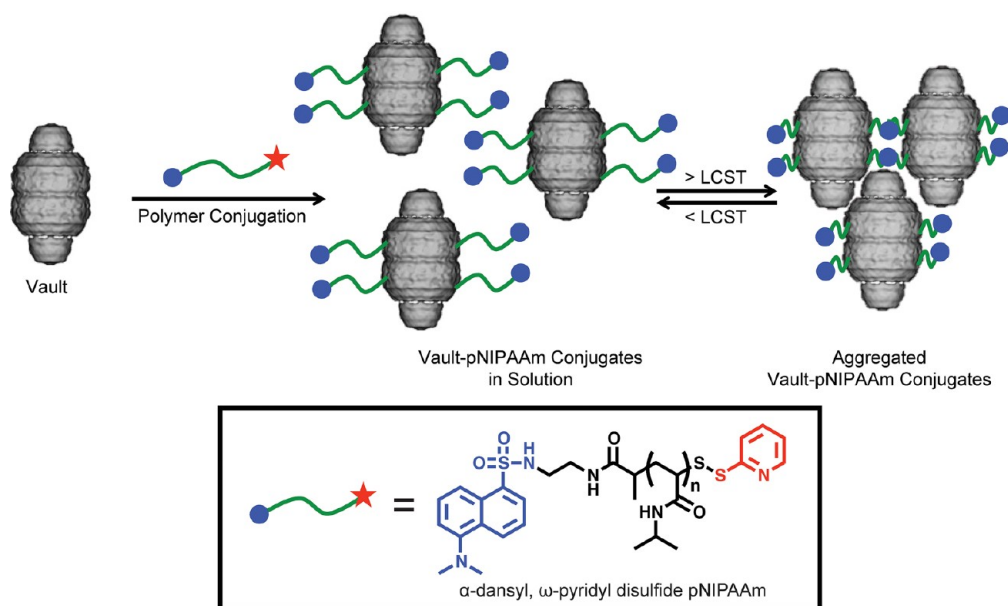
Smart polymers are responsive to external stimuli such as heat, pH, magnetic field, etc.,[22] and the analysis of the micro- and nanoassembly transitions has been undertaken.[23] Poly(N-isopropylacrylamide) (pNIPAAm) is a well-known temperature responsive smart polymer that undergoes a reversible phase transition, where it becomes insoluble in water above the lower critical solution temperature (LCST).[22] We and others have previously reported the preparation of protein-pNIPAAm conjugates,
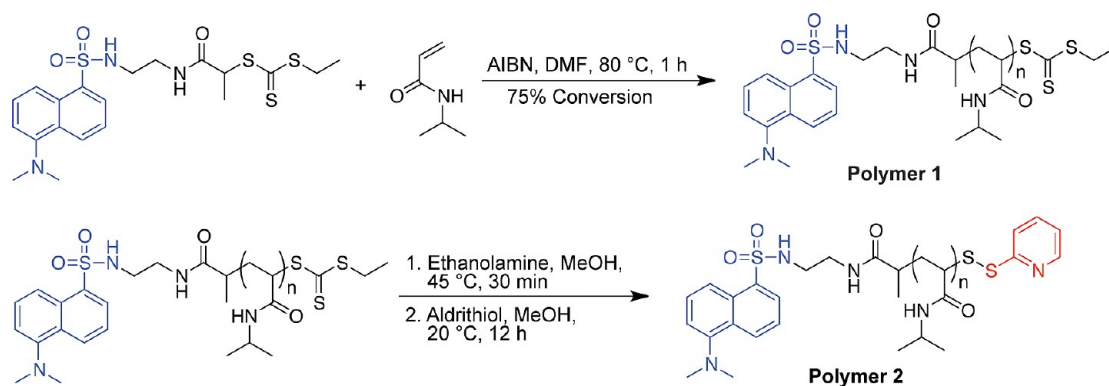
Scheme 1. Preparation of thermo-responsive vault-pNIPAAm conjugates. The vault image was adapted from cryoEM reconstructions of recombinant vaults. Adapted with permission from ref 31. Copyright 2006 American Chemical Society. (Cryo EM reconstruction of the vault - P. Stewart, Case Western Reserve University, Department of Pharmacology).

which exhibit the pNIPAAm phase behavior, while retaining the bioactivity of the protein.[24−30] Polymer conjugation results in altered properties upon exposure to heat. For example, ligand binding sites can be closed, proteins can be reversibly aggregated, and the polymer can be used to purify biomolecules by mild precipitation.[24,25,30] In this paper, we report that thermally responsive polymers can be added to vault nanocapsules without disrupting the structure of the particle.

First reported in 1986 by Rome and Kedersha, vaults are highly conserved ribonucleoprotein complexes found in high concentrations in almost all eukaryotic cells.[32−34] These massive particles weigh approximately 13 MDa and have a unique structure composed of a barrel waist and protruding caps at both ends (Scheme 1).[35] In recent years, high-resolution crystal structures have confirmed low resolution cryo-EM structures.[36] Naturally occurring vaults comprise several highly conserved proteins, with one protein, the 104 kDa major vault protein (MVP) accounting for over 70% of the vault mass. The MVP provides the basis for the vault structure, with ∼78 MVPs aligned from C- to N-terminus from the cap of the vault to the waist, with all of the N-termini facing toward the interior. Vaults are dynamic; the MVPs are noncovalently associated and although they bind to each other very tightly, they do have a kinetic off rate which means that dynamically they can open and close to accommodate small molecules which slip in or large proteins or other macromolecules which bind to their interior.[31] Vaults are also highly stable *in vivo* and *in vitro* to a variety of biological and physical stresses.[37]

Expression of MVP in insect cells results in the spontaneous assembly of non-native vault structures measuring 45 nm × 45 nm × 75 nm.[38] Although the natural biological function of vaults is unknown, recombinant vaults can be engineered for a variety of applications.[39] For example, the N-terminus of MVP can be modified to contain a cysteine-rich (4 cysteine residues) 12 amino acid peptide sequence to form CP-MVP. Vaults assembled from this fusion protein have increased particle stability.[39] Cell-specific targeting vaults have also been engineered by incorporating IgG binding peptides into recombinant MVPs for attachment of targeting antibodies.[40] While in nature vaults contain multiple copies of two large proteins (VPARP and TEP1) and one or more small vault RNAs (vRNAs), recombinant vaults have a hollow interior with an approximate volume of 5×10^7 Å^3, large enough to accommodate hundreds of proteins and many more small molecules.[31,35,41−43] For example, we have packaged gold nanoparticles and incorporated conducting polymers noncovalently into the vault interior.[42,43] In addition, a number of proteins have been packaged into the vault taking advantage of a binding site on MVP which faces the internal vault lumen. This site recognizes the vault protein VPARP through a protein domain at the VPARP C-terminus, which is referred to as INT for MVP *int*eraction domain.[39] INT fusion proteins bind with high affinity to the vault lumen, but they are slowly released. This strategy has been used to package antigens into vaults so that the vault can be used as an adjuvant and to package a chemokine, which activates the immune system.[44−46] Herein we report the feasibility of preparing smart vault nanoparticle conjugates by the synthesis of a vault-poly(N-isopropylacrylamide) conjugate. The synthesis and characterization of responsive properties are described.

Scheme 2. Synthesis of thiol-reactive pNIPAAm polymer.
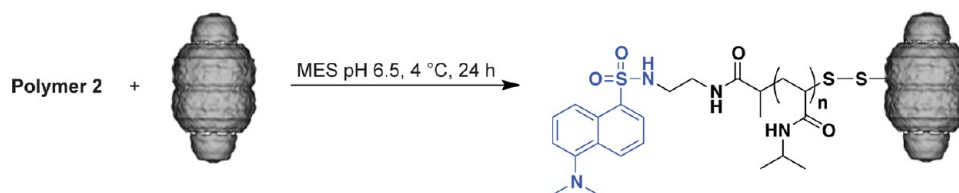
Scheme 3. Synthesis of CP-MVP vault-pNIPAAm conjugates.

RESULTS AND DISCUSSION

Our approach to developing thermo-responsive vault nanoparticles is based upon the conjugation of thiol-reactive pNIPAAm to cysteine-rich CP-MVP vaults. We and others have prepared cysteine-reactive polymers by reversible addition—fragmentation chain transfer (RAFT) polymerization.[47,48] RAFT is suitable for this application because it results in polymers with narrow molecular weight distributions.[49,50] Well-defined polymers are particularly important for this study because they exhibit sharp LCSTs. We chose to use a pyridyl-disulfide pNIPAAm in order to achieve reversible conjugation to the vault. We also introduced a dansyl group, a fluorophore, at the other end group for ease of visualization.

The polymer was prepared as shown in Scheme 2. First a dansyl-modified CTA was synthesized by coupling *N*-(2-aminoethyl)-5-(dimethylamino)naphthalene-1-sulfonamide with 2-(((ethylthio)carbonothioyl)thio)-propanoic acid (Supporting Information, Scheme S1 and ESI for synthesis details and characterization). The product was obtained in 64% yield. This CTA was then utilized in the RAFT polymerization of NIPAAm with AIBN in DMF at 80 °C. The polymerization was stopped after 1 h at 81% monomer conversion by ^{1}H NMR spectroscopy. Polymer **1** was obtained after extensive dialysis against MeOH. The number-average molecular weight (M_n) was determined by ^{1}H NMR (ESI, Supporting Information, Figure S3) to be 12.4 kDa and the polydispersity index (PDI) by GPC (ESI, Supporting Information, Figure S4) was 1.02. The trithiocarbonate end-group of **1** was transformed into a cysteine reactive pyridyl-disulfide *via* aminolysis of the trithiocarbonate to the free thiol with ethanolamine,

followed by an *in situ* disulfide exchange with Aldrithiol. After dialysis of the reaction mixture against MeOH, the α-dansyl, ω-pyridyl disulfide pNIPAAm, polymer **2**, was obtained. Molecular weight analysis indicated that the polymer had not coupled during the end group transformation because the M_n and PDI (12.4 kDa and 1.03, respectively) were the same as before the reaction (ESI, Supporting Information, Scheme S6). By comparing the integration of the peaks corresponding to the pyridyl disulfide to the dansyl group in the ^{1}H NMR spectrum (ESI, Figure S5), the conversion of the disulfide exchange was determined to be 81%.

Polymer **2** was conjugated to CP-MVP vault by incubating the CP-MVP vault at a ratio of 100:1 polymer/CP-MVP vault (Scheme 3). The resulting conjugate was analyzed by SDS-PAGE and compared to unmodified CP-MVP vault. Under nonreducing conditions there was a clear shift to higher molecular weight compared to the ~100 kDa CP-MVP vault (Scheme 1a, lanes 5 *versus* 4), and under reducing conditions, SDS-PAGE stained with coomassie blue showed no difference in molecular weight as expected because of the reversibility of the disulfide bond of the polymer connection (Figure 1a, lanes 2 and 3). Visualization of the gel with ultraviolet light confirmed conjugation; the dansyl fluorophore of the polymer overlaying with coomassie staining of the protein was clearly visible (Figure 1b, lane 3). The results demonstrate that the conjugate with the CP-MVP vault was prepared and that the conjugation was reversible.

The thermo-responsive properties of the conjugate were studied by UV—vis turbidity measurements. By UV—vis turbidity studies (Figure 2) **2** had an LCST of
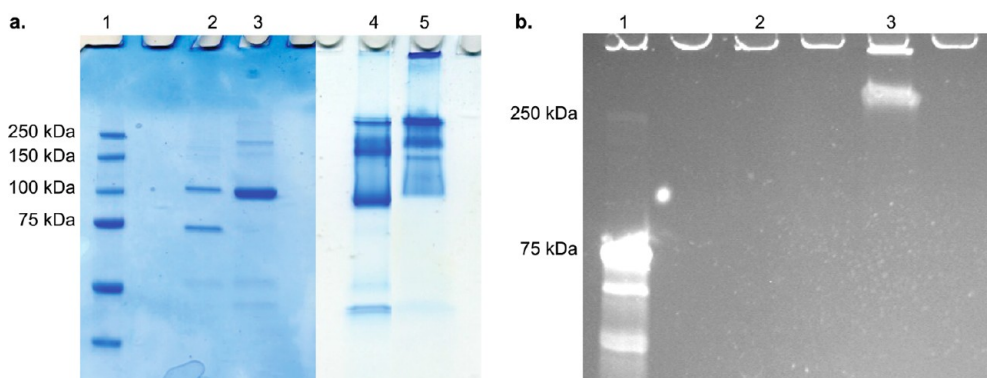
Figure 1. SDS-PAGE of CP-MVP vault and conjugate visualized by (a) coomassie blue staining (lane 1, protein marker; lane 2, CP-MVP vault reducing conditions; lane 3, Conjugate reducing conditions; lane 4, CP-MVP vault nonreducing conditions; lane 5, Conjugate nonreducing conditions) and (b) UV–vis excitation (lane 1, protein marker; lane 2, CP-MVP vault nonreducing conditions; lane 3, Conjugate nonreducing conditions).
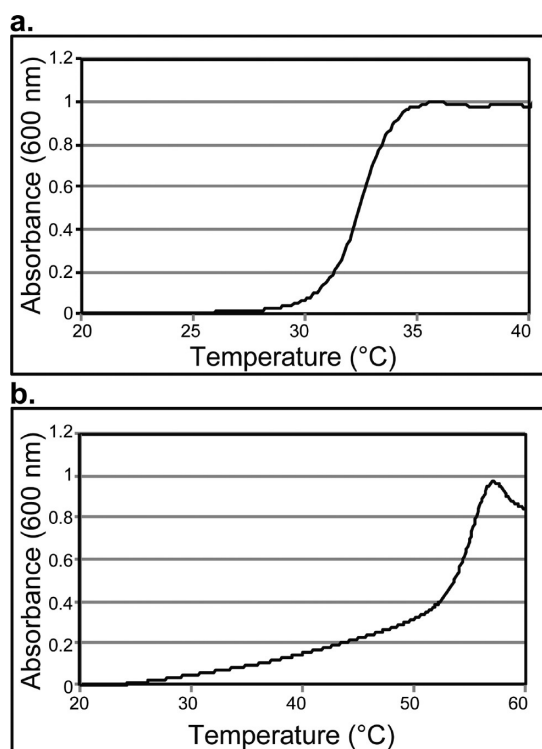

Figure 2. UV–vis turbidity study of (a) polymer 2 and (b) conjugate. LCST is 10% of the maximum absorbance.

30.5 °C. The phase transition was sharp, as expected for a narrow molecular weight distribution polymer. The hydrophobic dansyl group lowered the LCST from the typical value of 32 °C. Once the polymer was conjugated to the hydrophilic CP-MVP vault, the LCST was increased by the proximity of the hydrophilic protein to 35.9 °C. The phase transition was broad, potentially due to a distribution of number of polymers and attachment sites. The vault itself had no LCST as expected (ESI Supporting Information, Figure S7); no visible aggregation of the vault structure was observed up to at least 50 °C, indicating that the phase transition for the conjugate was due to the polymer. The results together confirmed that the polymer is covalently

attached to the protein and that the polymer confers thermal responsivity to the vault.

Dynamic light scattering (DLS) studies at different temperatures were performed to investigate the size of the conjugate (Figure 3). At 25 °C, the conjugate closely resembled the unmodified CP-MVP vault (49.7 nm ± 2.2 nm, versus 48.69 nm ± 0.44 nm, respectively). However upon heating to 40 °C, above the LCST of the polymer, the conjugate aggregated into micro-meter-sized particles, while the size of the unmodified CP-MVP vault did not change (53.98 nm ± 5.0). Inter-estingly, upon cooling the observed aggregates disap-peared and the conjugate returned to approximately its original size (58.76 nm ± 1.5 nm) suggesting that the aggregation was reversible.

This result was further investigated by electron micro-scopy. EM images of the conjugate and unmodified CP-MVP vault at 35 °C showed intact vault structures (Figure 4a,c, respectively). This indicated that modifi-cation of CP-MVP vaults with **2** did not alter the vault structure. However, when the samples were heated above the LCST to 45 °C, the conjugate appeared aggregated, yet with intact vault structures still re-cognizable within the aggregates (Figure 4d), while the unmodified CP-MVP vault structures were un-changed (Figure 4b). Interestingly, when the conju-gate was cooled back down to 4 °C, the vault struc-tures were no longer aggregated and looked the same as before heating (Figure 4e).

The data together demonstrate that conjugation of the pNIPAAm does not interfere with or disrupt vault structure. Yet, the polymer once attached allows for reversible aggregation of vaults without destroying their structure. This result is interesting because it implies that cargo could be potentially loaded within the vault, while the polymer could be used to precipi-tate the vaults at a site of interest. It is well-known that pNIPAAm can form aggregates at tumors, while remaining soluble in other tissue due to the differential in temperatures between the cancerous and normal
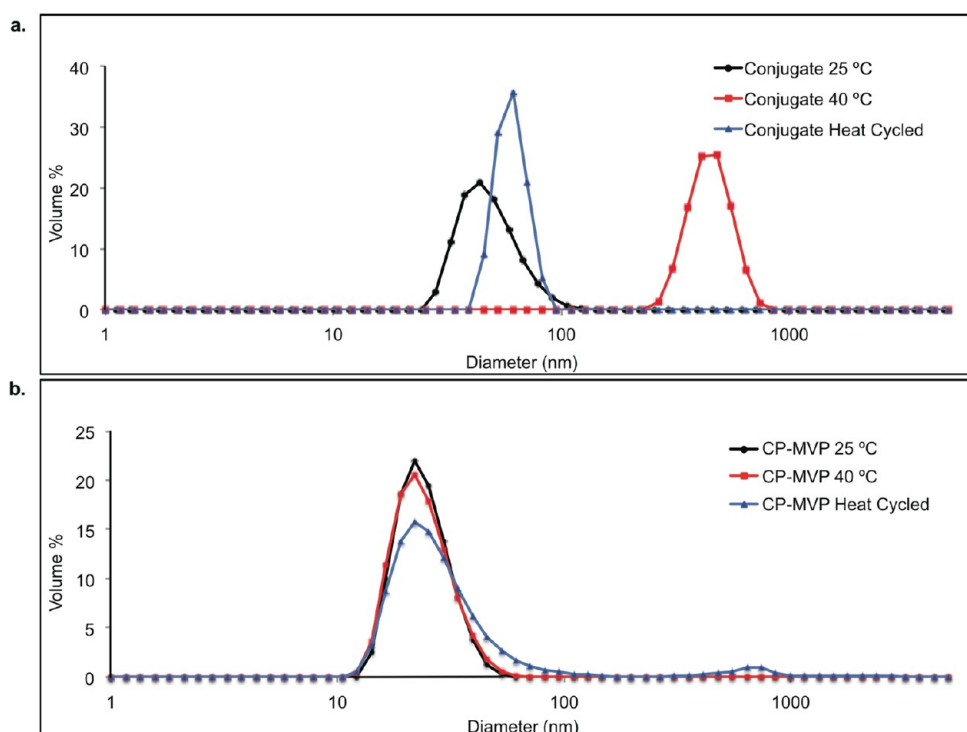
Figure 3. (a) DLS analysis of conjugate at 25 °C, 40 °C, and heat cycled (25 to 40 °C to 25 °C) conjugate cooled to 25 °C. (b) DLS analysis of unmodified CP-MVP vaults at 25 °C, 40 °C, and heat cycled (25 to 40 °C to 25 °C).
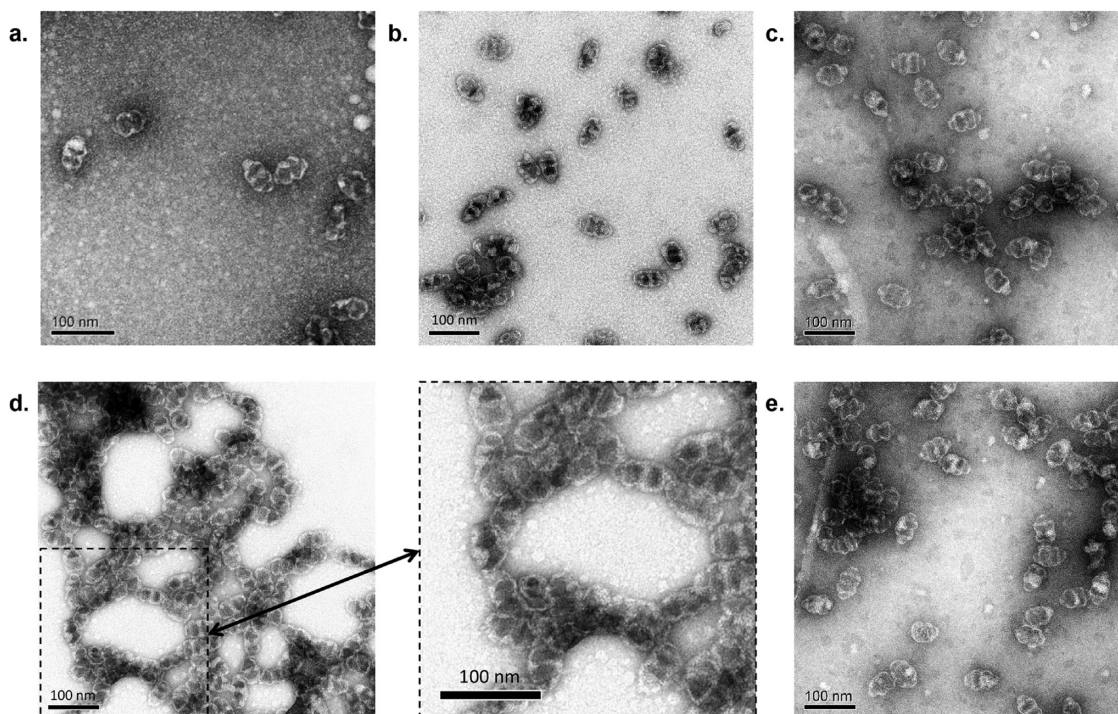

Figure 4. Negative stain TEM of unmodified CP-MVP vaults at (a) 35 °C and (b) 45 °C; 2-CP-MVP vault conjugates at (c) 35 °C, (d) 45 °C (inset image at the bottom middle indicated by the arrow is an expanded view of the dashed box in panels d and e after cooling back down to 4 °C.

tissues.[51,52] An aggregating vault conjugate would potentially undergo similar selectivity, yet at the same time allow for protein or drug delivery from the vault nanocapsules. Drug loading and delivery within the

vault is possible, and has been demonstrated with vaults engineered to contain lipids.[39]

It is not known if the pNIPAAm is attached to the cysteine-rich region at the N-terminus in the interior or

to free cysteines at the exterior. Upon examination of the crystal structure of the rat MVP,[33] there are six cysteines on the exterior of the vault; however, all but one appear to be not surface accessible. Cysteine 356 may be exposed or at least partially exposed. CP-MVP is engineered to contain an additional four cysteines near the N-terminus of the protein, which is in the interior of the vault. Owing to the dynamic nature of the CP-MVP vaults, the polymer should be able to enter the structure to react. Thus, likely the polymer is attached to both the exterior and interior. It also may be possible that the polymer in the interior could thread out and participate in aggregation of the vaults. Our initial attempts to investigate the location(s) of the chains were to associate gold nanoparticle-modified streptavidin with polymers that had biotin groups instead of a dansyl (data not shown). However, the location of the polymer was unclear. Cysteine mutagenesis experiments may provide the desired information. Yet, it is clear from the results that attachment of the polymer inside the vault does not disrupt the structure, as full vault structures were observed. The results also demonstrate that conjugates with pNIPAAm that contain a fluorophore can be synthesized. This implies that other end groups could be prepared, and multifunctional vaults could be made with this strategy. Vaults are stable, nonimmunogenic, readily engineered, and expressed, making them a versatile platform for the development of sophisticated hybrid nanomaterials. Thus, we envision that the thermally responsive vaults described herein are an interesting and versatile nanoplatform for drug delivery and other applications.

CONCLUSION

Novel biohybrid nanoparticles have been synthesized through covalent conjugation of pNIPAAm to recombinant CP-MVP vaults. Pyridyl disulfide pNIPAAm with a dansyl group at the other end group was conjugated to CP-MVP vaults via reaction with free cysteines. The resulting conjugates were thermally responsive. UV–vis turbidity measurements showed that the conjugates had an LCST. DLS studies demonstrated that upon heating, aggregates formed, which were reversible with cooling. This result was confirmed by EM studies, whereby a reversible aggregation of polymer-modified vaults was observed, while the vault nanocapsules remained intact regardless of the temperature. We envision that these smart vault conjugates may be used for drug delivery applications in conjunction with previously reported vault-based hydrophobic drug delivery methods and emerging in vivo localized heating techniques[41,53,54] to build up depots of therapeutic drugs in tumors for a sustained release of drugs to tumor cells, and other interesting medical and biotechnology applications.

METHODS

Materials. Chemicals were purchased from Sigma-Aldrich, Fisher Scientific, and Acros. AIBN was recrystallized twice from acetone. NIPAAm was recrystallized twice from hexanes. Rat CP-MVP was expressed from a baculovirus system in *Sf9* insect cells, which do not contain endogenous vaults according to our literature procedure.[39]

Instrumental. NMR spectra were obtained on a Bruker 600 MHz DRX spectrometer. Proton NMR spectra were acquired with a relaxation delay of 30 s for all polymers. UV–vis spectra were obtained on a Biomate 5 Thermo Spectronic UV–vis spectrometer and a Hewlett-Packard HP8453 diode-array UV–vis spectrophotometer with Peltier temperature control spectrometer with quartz cells. GPC was conducted on a Shimadzu HPLC system equipped with a refractive index detector RID-10A, one Polymer Laboratories PLgel guard column, and two Polymer Laboratories PLgel 5 μm mixed D columns. LiBr (0.1 M) in DMF at 40 °C was used as an eluent (flow rate: 0.80 mL/min). Calibration was performed using near-monodisperse PMMA standards from Polymer Laboratories. DLS was performed on a Malvern Zetasizer Nano-S. SDS-PAGE was performed using Bio-Rad Any kD Mini-PROTEAN-TGX gels.

Polymerization of NIPAAm in the Presence of Dansyl CTA To Afford α-Dansyl pNIPAAm. The dansyl CTA (46 mg, 0.095 mmol), NIPAAm (1.4 g, 12.0 mmol), and AIBN (1.6 mg, 0.113 mmol), were added to a Schlenk tube containing a stirring bar, and DMF (1.9 mL) was added to dissolve the solids. Freeze–pump–thaw cycles were repeated five times and the reaction was performed at 70 °C in an oil bath. The reaction was stopped after 1 h at 81% monomer conversion by cooling with liquid nitrogen and exposing the reaction to atmosphere. Polymer **1** was purified by dialyzing against MeOH (MWCO 3500 g/mol) giving the α-dansyl pNIPAAm. ^{1}H NMR (600 MHz, MeOD) δ: 8.55 (d), 8.36–8.28 (m), 8.24–8.15 (m), 8.12–7.35 (NH, pNIPAAM), 7.26 (d), 4.60 (s), 4.13–3.77 (bs), 3.43–3.23 (m), 2.86 (s), 2.25–1.80 (CH, pNIPAAm), 1.78–1.45 (CH$_2$, pNIPAAm), 1.26–0.93 (NCH$_3$, pNIPAAm). M_n by ^{1}H NMR was 12 400 g/mol (targeted 12 000 g/mol). M_n(GPC) was 14 200 g/mol and the PDI was 1.02.

In Situ Aminolysis and Disulfide Exchange of Dansyl pNIPAAm with Aldrithiol To Form polymer 2. **1** (70 mg, 0.005 mmol) was added to a Schlenk tube equipped with a stirring bar and dissolved in MeOH (0.7 mL). In a second Schlenk tube equipped with a stirring bar, ethanolamine (14 μg, 0.230 μmol) was added. In a third Schlenk tube equipped with a stirring bar, Aldrithiol (75 mg, 0.340 mmol) was dissolved in MeOH (0.7 mL). All three Schlenk tubes were subjected to five freeze–pump–thaw cycles. The contents of the first Schlenk tube, containing α-dansyl pNIPAAm and MeOH, were then transferred into the second Schlenk tube, containing ethanolamine, using a syringe. The second Schlenk tube was then immersed in an oil bath at 45 °C and the solution was allowed to stir. After 30 min, the second Schlenk tube was removed from the oil bath and the contents, dansyl pNIPAAm, MeOH, and ethanolamine, were transferred to the third Schlenk tube, containing Aldrithiol and MeOH, via syringe. The third Schlenk tube containing dansyl pNIPAAm, ethanolamine, Aldrithiol and MeOH was stirred at 20 °C for 12 h. The product was purified by dialyzing against MeOH (MWCO 3500 g/mol) giving polymer **2**. End-group conversion of the trithiocarbonate to a pyridyl disulfide was 81% by ^{1}H NMR. ^{1}H NMR (600 MHz, MeOD) δ: 8.55 (d, Ar CH), 8.40–8.27 (m, Ar CH), 8.24–8.14 (NH, pNIPAAm), 7.26 (Ar CH), 7.22–7.15 (Ar CH), 3.95 (CH$_3$, pNIPAAm), 3.45–3.20 (CH$_2$CH$_2$), 2.87 (NCH$_3$), 2.34–1.76 (CH, pNIPAAm), 1.76–1.46 (CH$_2$, pNIPAAM), 1.26–1.20 (NCH$_3$, pNIPAAm). M_n (^{1}H NMR) = 12 400 g/mol; M_n (GPC) = 14 200 g/mol; PDI = 1.03.

pNIPAAm Conjugation to CP-MVP. A pH 6.5 20 mM 2-(N-morpholino) ethanesulfonic acid) (MES) buffer was degassed

with argon gas for 30 min. CP-MVP (0.50 mg, 0.05 μmol) in 250 μL of buffer was treated with triscarboxylethylphosphine (TCEP) resin for 2 h at 4 °C, then filtered through a 0.22 μm syringe filter. **2** (6.20 mg, 5.00 μmol) was dissolved in 250 μL of buffer. The filtered CP-MVP solution was added to the solution containing **2**. The reaction was allowed to stand at 4 °C for 24 h before purification by ultrafiltration (MWCO 100 000 g/mol) to give the conjugate.

LCST Determination. A solution of the polymer, conjugate, or unmodified CP-Vault-pNIPAAm conjugate at a concentration of 1 mg mL^{-1} in pH 6.5 20 mM MES was placed in a 100 μL quartz cuvette. The cuvette was placed in a Hewlett-Packard HP8453 diode-array UV–vis spectrophotometer with Peltier temperature control. The following temperature program was used: temperature was elevated at 0.5 °C min^{-1} and held for 30 s prior to measuring the absorbance at 600 nm. The LCST was determined at 10% of the maximum absorbance.

DLS Size Determination. A solution of CP-Vault-pNIPAAm conjugate at a concentration of 1 mg mL^{-1} in pH 6.5, 20 mM MES was placed in a 40 μL disposable cuvette. The cuvette was placed in a Malvern Zetasizer Nano-S. The temperature was allowed to equilibrate for three minutes before beginning the DLS measurement. This process was repeated three times, sizes are reported as an average of three measurements.

Preparation of the TEM Sample. A 40 μL aliquot of a 0.2 μg μL^{-1} solution of CP-Vault-pNIPAAm conjugate was warmed to a set temperature (35 or 45 °C or heated to 45 °C then cooled to 4 °C) and incubated for 7 min. A 20 μL aliquot of each solution was then pipetted onto the surface of a heating block at the set temperature. A carbon-coated EM grid was floated up-side down on the sample to allow the conjugate to adsorb to the grid surface. After 7 min, the grid was removed from the sample and blotted on filter paper to remove excess liquid. The grid was then floated up-side down in 500 μL of a 1% uranyl acetate solution at the set temperatures. After 7 min, the grid was removed from the uranyl acetate solution and blotted on filter paper. TEM was conducted on a JEOL JEM1200-EX transmission electron microscope. Images were taken using a Gatan BioScan 600W 1 × 1K digital camera and Digital Micrograph acquisition software.

Conflict of Interest: The authors declare no competing financial interest.

Supporting Information Available: Synthesis and NMR spectra of the dansyl CTA, polymer NMR spectra, and GPC traces, UV–vis turbidity study of CP-MVP vaults. This material is available free of charge *via* the Internet at http://pubs.acs.org.

REFERENCES AND NOTES

1. Douglas, T.; Young, M. Virus Particles as Templates for Materials Synthesis. *Adv. Mater.* **1999**, *11*, 679–681.
2. Witus, L. S.; Francis, M. B. Using Synthetically Modified Proteins to Make New Materials. *Acc. Chem. Res.* **2011**, *44*, 774–783.
3. Lee, L. A.; Niu, Z. W.; Wang, Q. Viruses and Virus-like Protein Assemblies-Chemically Programmable Nanoscale Building Blocks. *Nano Res.* **2009**, *2*, 349–364.
4. Uchida, M.; Klem, M. T.; Allen, M.; Suci, P.; Flenniken, M.; Gillitzer, E.; Varpness, Z.; Liepold, L. O.; Young, M.; Douglas, T. Biological Containers: Protein Cages as Multifunctional Nanoplatforms. *Adv. Mater.* **2007**, *19*, 1025–1042.
5. Soto, C. M.; Ratna, B. R. Virus Hybrids as Nanomaterials for Biotechnology. *Curr. Opin. Biotechnol.* **2010**, *21*, 426–438.
6. Jutz, G.; Boker, A. Bionanoparticles as Functional Macromolecular Building Blocks—A New Class of Nanomaterials. *Polymer* **2011**, *52*, 211–232.
7. Steinmetz, N. F.; Evans, D. J. Utilisation of Plant Viruses in Bionanotechnology. *Org. Biomol. Chem.* **2007**, *5*, 2891–2902.
8. Endo, M.; Fujitsuka, M.; Majima, T. Porphyrin Light-Harvesting Arrays Constructed in the Recombinant Tobacco Mosaic Virus Scaffold. *Chem.—Eur. J.* **2007**, *13*, 8660–8666.
9. Nam, K. T.; Kim, D.-W.; Yoo, P. J.; Chiang, C.-Y.; Meethong, N.; Hammond, P. T.; Chiang, Y.-M.; Belcher, A. M. Virus-Enabled Synthesis and Assembly of Nanowires for Lithium Ion Battery Electrodes. *Science* **2006**, *312*, 885–888.
10. Comellas-Aragones, M.; Engelkamp, H.; Claessen, V. I.; Sommerdijk, N.; Rowan, A. E.; Christianen, P. C. M.; Maan, J. C.; Verduin, B. J. M.; Cornelissen, J. J. L. M.; Nolte, R. J. M. A Virus-Based Single-Enzyme Nanoreactor. *Nat. Nanotechnol.* **2007**, *2*, 635–639.
11. Minten, I. J.; Claessen, V. I.; Blank, K.; Rowan, A. E.; Nolte, R. J. M.; Cornelissen, J. J. L. M. Catalytic Capsids: The Art of Confinement. *Chem. Sci.* **2011**, *2*, 358–362.
12. Patterson, D. P.; Prevelige, P. E.; Douglas, T. Nanoreactors by Programmed Enzyme Encapsulation inside the Capsid of the Bacteriophage P22. *ACS Nano* **2012**, *6*, 5000–5009.
13. MaHam, A.; Tang, Z. W.; Wu, H.; Wang, J.; Lin, Y. H. Protein-Based Nanomedicine Platforms for Drug Delivery. *Small* **2009**, *5*, 1706–1721.
14. Manchester, M.; Singh, P. Virus-Based Nanoparticles (VNPS): Platform Technologies for Diagnostic Imaging. *Adv. Drug Delivery Rev.* **2006**, *58*, 1505–1522.
15. Ma, Y. J.; Nolte, R. J. M.; Cornelissen, J. J. L. M. Virus-Based Nanocarriers for Drug Delivery. *Adv. Drug Delivery Rev.* **2012**, *64*, 811–825.
16. Garcea, R. L.; Gissmann, L. Virus-like Particles as Vaccines and Vessels for the Delivery of Small Molecules. *Curr. Opin. Biotechnol.* **2004**, *15*, 513–517.
17. Raja, K. S.; Wang, Q.; Gonzalez, M. J.; Manchester, M.; Johnson, J. E.; Finn, M. G. Hybrid Virus-Polymer Materials. 1. Synthesis and Properties of PEG-Decorated Cowpea Mosaic Virus. *Biomacromolecules* **2003**, *4*, 472–476.
18. Schlick, T. L.; Ding, Z.; Kovacs, E. W.; Francis, M. B. Dual-Surface Modification of the Tobacco Mosaic Virus. *J. Am. Chem. Soc.* **2005**, *127*, 3718–3723.
19. O'Riordan, C. R.; Lachapelle, A.; Delgado, C.; Parkes, V.; Wadsworth, S. C.; Smith, A. E.; Francis, G. E. Pegylation of Adenovirus with Retention of Infectivity and Protection from Neutralizing Antibody *in Vitro* and *in Vivo*. *Hum. Gene Ther.* **1999**, *10*, 1349–1358.
20. Sikkema, F. D.; Comellas-Aragones, M.; Fokkink, R. G.; Verduin, B. J. M.; Cornelissen, J. J. L. M.; Nolte, R. J. M. Monodisperse Polymer-Virus Hybrid Nanoparticles. *Org. Biomol. Chem.* **2007**, *5*, 54–57.
21. Lucon, J.; Qazi, S.; Uchida, M.; Bedwell, G. J.; LaFrance, B.; Prevelige, P. E.; Douglas, T. Use of the Interior Cavity of the P22 Capsid for Site-Specific Initiation of Atom-Transfer Radical Polymerization with High-Density Cargo Loading. *Nat. Chem.* **2012**, *4*, 781–788.
22. Alarcon, C. d. l. H.; Pennadam, S.; Alexander, C. Stimuli Responsive Polymers for Biomedical Applications. *Chem. Soc. Rev.* **2005**, *34*, 276–285.
23. Antipina, M. N.; Sukhorukov, G. B. Remote Control over Guidance and Release Properties of Composite Polyelectrolyte Based Capsules. *Adv. Drug Delivery Rev.* **2011**, *63*, 716–729.
24. Chen, G. H.; Hoffman, A. S. Preparation and Properties of Thermoreversible, Phase-Separating Enzyme-Oligo(N-Isopropylacrylamide) Conjugates. *Bioconjugate Chem.* **1993**, *4*, 509–514.
25. Stayton, P. S.; Shimoboji, T.; Long, C.; Chilkoti, A.; Chen, G. H.; Harris, J. M.; Hoffman, A. S. Control of Protein-Ligand Recognition Using a Stimuli-Responsive Polymer. *Nature* **1995**, *378*, 472–474.
26. Heredia, K. L.; Bontempo, D.; Ly, T.; Byers, J. T.; Halstenberg, S.; Maynard, H. D. *In Situ* Preparation of Protein—"Smart" Polymer Conjugates with Retention of Bioactivity. *J. Am. Chem. Soc.* **2005**, *127*, 16955–16960.
27. Heredia, K. L.; Grover, G. N.; Tao, L.; Maynard, H. D. Synthesis of Heterotelechelic Polymers for Conjugation of Two Different Proteins. *Macromolecules* **2009**, *42*, 2360–2367.

28. Tao, L.; Kaddis, C. S.; Loo, R. R. O.; Grover, G. N.; Loo, J. A.; Maynard, H. D. Synthesis of Maleimide-End-Functionalized Star Polymers and Multimeric Protein-Polymer Conjugates. *Macromolecules* **2009**, *42*, 8028–8033.

29. Vazquez-Dorbatt, V.; Tolstyka, Z. P.; Maynard, H. D. Synthesis of Aminooxy End-Functionalized pNIPAAm by RAFT Polymerization for Protein and Polysaccharide Conjugation. *Macromolecules* **2009**, *42*, 7650–7656.

30. Chang, C.-W.; Nguyen, T. H.; Maynard, H. D. Thermoprecipitation of Glutathione S-Transferase by Glutathione-Poly-(*N*-Isopropylacrylamide) Prepared by RAFT Polymerization. *Macromol. Rapid Commun.* **2010**, *31*, 1691–1695.

31. Poderycki, M. J.; Kickhoefer, V. A.; Kaddis, C. S.; Raval-Fernandes, S.; Johansson, E.; Zink, J. I.; Loo, J. A.; Rome, L. H. The Vault Exterior Shell Is a Dynamic Structure That Allows Incorporation of Vault-Associated Proteins into Its Interior. *Biochemistry* **2006**, *45*, 12184–12193.

32. Kedersha, N. L.; Rome, L. H. Isolation and Characterization of a Novel Ribonucleoprotein Particle—Large Structures Contain a Single Species of Small RNA. *J. Cell Biol.* **1986**, *103*, 699–709.

33. Kedersha, N. L.; Miquel, M. C.; Bittner, D.; Rome, L. H. Vaults 2. Ribonucleoprotein Structures Are Highly Conserved among Higher and Lower Eukaryotes. *J. Cell Biol.* **1990**, *110*, 895–901.

34. Suprenant, K. A. Vault Ribonucleoprotein Particles: Sarcophagi, Gondolas, or Safety Deposit Boxes? *Biochemistry* **2002**, *41*, 14447–14454.

35. Kong, L. B.; Siva, A. C.; Rome, L. H.; Stewart, P. L. Structure of the Vault, a Ubiquitous Cellular Component. *Struct. Fold. Des.* **1999**, *7*, 371–379.

36. Tanaka, H.; Kato, K.; Yamashita, E.; Sumizawa, T.; Zhou, Y.; Yao, M.; Iwasaki, K.; Yoshimura, M.; Tsukihara, T. The Structure of Rat Liver Vault at 3.5 Angstrom Resolution. *Science* **2009**, *323*, 384–388.

37. Esfandiary, R.; Kickhoefer, V. A.; Rome, L. H.; Joshi, S. B.; Middaugh, C. R. Structural Stability of Vault Particles. *J. Pharm. Sci.* **2009**, *98*, 1376–1386.

38. Stephen, A. G.; Raval-Fernandes, S.; Huynh, T.; Torres, M.; Kickhoefer, V. A.; Rome, L. H. Assembly of Vault-like Particles in Insect Cells Expressing Only the Major Vault Protein. *J. Biol. Chem.* **2001**, *276*, 23217–23220.

39. Kickhoefer, V. A.; Garcia, Y.; Mikyas, Y.; Johansson, E.; Zhou, J. C.; Raval-Fernandes, S.; Minoofar, P.; Zink, J. I.; Dunn, B.; Stewart, P. L.; *et al*. Engineering of Vault Nanocapsules with Enzymatic and Fluorescent Properties. *Proc. Natl. Acad. Sci. U.S.A.* **2005**, *102*, 4348–4352.

40. Kickhoefer, V. A.; Han, M.; Raval-Fernandes, S.; Poderycki, M. J.; Moniz, R. J.; Vaccari, D.; Silvestry, M.; Stewart, P. L.; Kelly, K. A.; Rome, L. H. Targeting Vault Nanoparticles to Specific Cell Surface Receptors. *ACS Nano* **2009**, *3*, 27–36.

41. Buehler, D. C.; Toso, D. B.; Kickhoefer, V. A.; Zhou, Z. H.; Rome, L. H. Vaults Engineered for Hydrophobic Drug Delivery. *Small* **2011**, *7*, 1432–1439.

42. Goldsmith, L. E.; Pupols, M.; Kickhoefer, V. A.; Rome, L. H.; Monbouquette, H. G. Utilization of a Protein "Shuttle" to Load Vault Nanocapsules with Gold Probes and Proteins. *ACS Nano* **2009**, *3*, 3175–3183.

43. Ng, B. C.; Yu, M.; Gopal, A.; Rome, L. H.; Monbouquette, H. G.; Tolbert, S. H. Encapsulation of Semiconducting Polymers in Vault Protein Cages. *Nano Lett.* **2008**, *8*, 3503–3509.

44. Champion, C. I.; Kickhoefer, V. A.; Liu, G. C.; Moniz, R. J.; Freed, A. S.; Bergmann, L. L.; Vaccari, D.; Raval-Fernandes, S.; Chan, A. M.; Rome, L. H.; (et al). A Vault Nanoparticle Vaccine Induces Protective Mucosal Immunity. *PLOS One* **2009**, *4*, e5409.

45. Kar, U. K.; Jiang, J. N.; Champion, C. I.; Salehi, S.; Srivastava, M.; Sharma, S.; Rabizadeh, S.; Niazi, K.; Kickhoefer, V.; Rome, L. H.; *et al*. Vault Nanocapsules as Adjuvants Favor Cell-Mediated over Antibody-Mediated Immune Responses Following Immunization of Mice. *PLOS One* **2012**, *7*, e38553.

46. Kar, U. K.; Srivastava, M. K.; Andersson, A.; Baratelli, F.; Huang, M.; Kickhoefer, V. A.; Dubinett, S. M.; Rome, L. H.; Sharma, S. Novel Ccl21-Vault Nanocapsule Intratumoral Delivery Inhibits Lung Cancer Growth. *PLOS One* **2011**, *6*, e18758.

47. Boyer, C.; Bulmus, V.; Davis, T. P.; Ladmiral, V.; Liu, J.; Perrier, S. Bioapplications of RAFT Polymerization. *Chem. Rev.* **2009**, *109*, 5402–5436.

48. Grover, G. N.; Maynard, H. D. Protein−Polymer Conjugates: Synthetic Approaches by Controlled Radical Polymerizations and Interesting Applications. *Curr. Opin. Chem. Biol.* **2010**, *14*, 818–827.

49. Chiefari, J.; Chong, Y. K.; Ercole, F.; Krstina, J.; Jeffery, J.; Le, T. P. T.; Mayadunne, R. T. A.; Meijs, G. F.; Moad, C. L.; Moad, G.; *et al*. Living Free-Radical Polymerization by Reversible Addition-Fragmentation Chain Transfer: The RAFT Process. *Macromolecules* **1998**, *31*, 5559–5562.

50. Moad, G.; Rizzardo, E.; Thang, S. H. Living Radical Polymerization by the RAFT Process—A Third Update. *Aust. J. Chem.* **2012**, *65*, 985–1076.

51. Bawa, P.; Pillay, V.; Choonara, Y. E.; Toit, L. C. d. Stimuli-Responsive Polymers and Their Applications in Drug Delivery. *Biomed. Mater.* **2009**, *4*, 022001.

52. Xu, J.; Liu, S. Y. Polymeric Nanocarriers Possessing Thermo-responsive Coronas. *Soft Matter* **2008**, *4*, 1745–1749.

53. Meyer, D. E.; Shin, B. C.; Kong, G. A.; Dewhirst, M. W.; Chilkoti, A. Drug Targeting Using Thermally Responsive Polymers and Local Hyperthermia. *J. Controlled Release* **2001**, *74*, 213–224.

54. Skirtach, A. G.; Javier, A. M.; Kreft, O.; Kohler, K.; Alberola, A. P.; Mohwald, H.; Parak, W. J.; Sukhorukov, G. B. Laser-Induced Release of Encapsulated Materials inside Living Cells. *Angew. Chem.-Int. Ed.* **2006**, *45*, 4612–4617.